

High-temperature phase transitions in SrZrO₃

Brendan J. Kennedy and Christopher J. Howard*
School of Chemistry, The University of Sydney, Sydney, NSW 2006 Australia

Bryan C. Chakoumakos
Solid State Division, Oak Ridge National Laboratory, Oak Ridge, Tennessee 37831
 (Received 30 July 1998)

The high-temperature phase transitions of SrZrO₃ have been studied using powder neutron diffraction and the Rietveld method. The material is tetragonal (*I4/mcm*) between ~1020 and 1360 K. At higher temperatures (>1360 K) the structure was found to be the ideal cubic perovskite (*Pm* $\bar{3}$ *m*). From the neutron-diffraction data and the space-group assignments, the transition from the tetragonal to cubic phase is consistent with a continuous phase transition. The angle of tilt of the oxygen octahedron in the tetragonal phase is taken to be the order parameter and its temperature variation is typical of a tricritical phase transition.

[S0163-1829(99)05805-1]

INTRODUCTION

A number of ABO₃-type oxides that adopt the orthorhombic GdFeO₃-type structure under ambient conditions undergo structural transitions to the archetypal cubic perovskite structure at elevated temperatures.¹ One of the best-studied examples is SrZrO₃, which is reported to undergo at least three phase transitions as follows:²⁻⁵ Orthorhombic(*Pnma*)→orthorhombic(*Cmcm*)→tetragonal (*I4/mcm*)→cubic(*Pm* $\bar{3}$ *m*) at 970 K, 1100 K, and 1440 K, respectively.

The degree of distortion of these perovskites may be described by tilting of the BO₆ octahedra, and even where a structural transition is not observed the tilt angle decreases as the temperature increases. A number of workers have used such changes to infer the presence of thermally induced phase transitions.⁶

Despite the importance of many perovskite-type oxides under nonambient conditions, for example MgSiO₃ as it occurs in the earth's mantle, or CaTiO₃ which is a key component of Synroc used to immobilize nuclear waste,⁷ only a limited number of accurate high-temperature structural studies on perovskites have been reported.⁸⁻¹² Consequently it is not yet possible to identify any systematics in the thermal behavior of the GdFeO₃-type perovskites.

Recently Howard and Stokes¹³ used group-theoretical analysis to describe the relationship between the various structures derived from the aristotype cubic perovskite by the tilting of rigid octahedral units. This analysis suggested possible pathways by which the phase transitions could occur. The analysis showed that the transitions from *Pm* $\bar{3}$ *m* to *I4/mcm* and then to *Cmcm* could be continuous however, there is no continuous path for the transition from *Cmcm* to *Pnma*.

We therefore sought to confirm the pathway for the conversion of SrZrO₃ from orthorhombic (*Pnma*) to cubic (*Pm* $\bar{3}$ *m*) and to better characterize the tetragonal-to-cubic transformation. The present paper reports new data on the evolution of the crystal structure of SrZrO₃ at high tempera-

ture using powder neutron diffraction and the Rietveld method for data analysis.

EXPERIMENTAL

Powder samples of SrZrO₃ were obtained from Aldrich chemicals and used as received. The neutron powder-diffraction patterns were recorded using neutrons of wavelength 1.5005 Å, in 0.05° steps over the range 11° < 2θ < 135° on the powder diffractometer on HB4 at the High Flux Isotope Reactor at Oak Ridge National Laboratory.¹⁴ The sample was compacted into a cylinder and placed in a thin-walled 9-mm-diameter vanadium can. The sample assembly was housed in an ILL-type vacuum furnace under a dynamic vacuum of around 10⁻⁶ torr. The data were collected first at room temperature and then at successively higher temperatures. The structural refinements were undertaken using the Rietveld program LHPM operating on a PC.¹⁵ The background was defined by a third-order polynomial in 2θ and was refined simultaneously with the other profile parameters. A Voigt function was chosen to generate the line shape of the neutron-diffraction peaks where the width of the Gaussian component was varied according to full width at half maximum, (FWHM)² = U tan² θ + V tan θ + W to describe instrumental and strain broadening and that of the Lorentzian component as η sec θ to model broadening due to particle size. The 2θ region near 38° affected by a peak from the furnace heating element was excluded from the refinements.

RESULTS AND DISCUSSION

Thermal behavior

Examination of the powder neutron diffraction data confirmed the following sequence of phase transitions: orthorhombic (*Pnma*)→orthorhombic (*Cmcm*)→tetragonal (*I4/mcm*)→cubic (*Pm* $\bar{3}$ *m*), where the tetragonal (*I4/mcm*) phase exists over a reasonably wide temperature range from about 1023 to 1353 K. The temperature variations of the cell parameters and volume are shown in

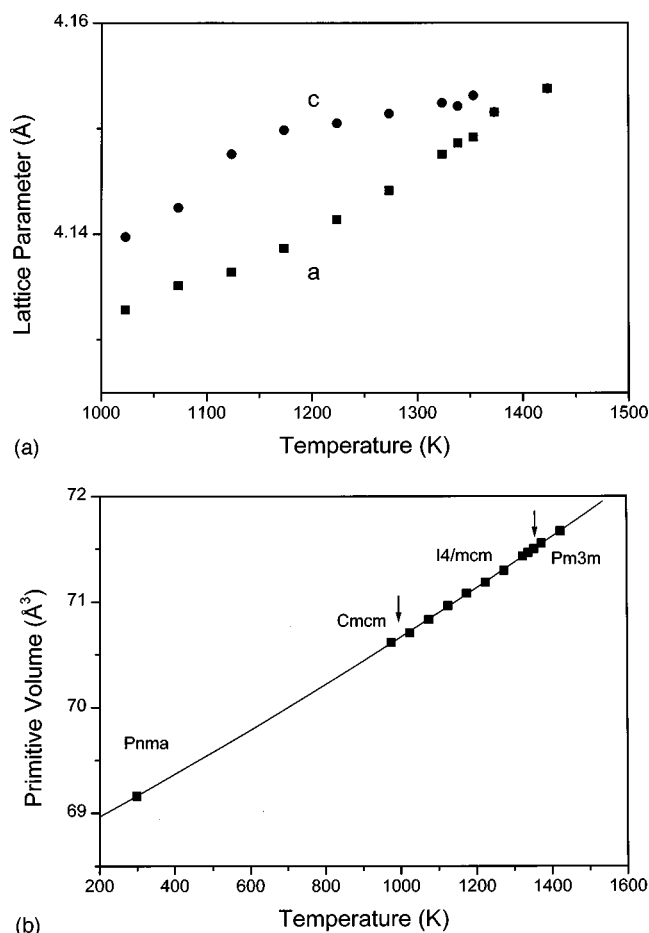


FIG. 1. Temperature dependence of (a) the normalized lattice parameters for SrZrO_3 (b) the volume of the primitive cell for SrZrO_3 . The data were collected while heating the sample except for the point at 1223 K that was collected during a cooling cycle.

Fig. 1. The identification of the appropriate symmetry involved a careful examination of the various, weak, superstructure peaks that are a result of tilting of the octahedra. Figure 2 illustrates some of the weak reflections that are diagnostic of the different phases.

Orthorhombic structure (*Pnma*)

Under ambient conditions SrZrO_3 is reported to be isostructural with the mineral perovskite and has a $\sqrt{2}a \times \sqrt{2}a \times 2a$ orthorhombic superstructure.³ For consistency with other studies of GdFeO_3 -type perovskites the structure was refined in the alternate setting, *Pbnm* giving the following atom positions: Sr 4c (0.0040, 0.5242, 1/4) Zr 4a (0,0,0) O(1) 4c (-0.0687, -0.0133, 1/4), and O(2) 8d (0.2154, 0.2837, 0.0363) and $a = 5.7963$ $b = 5.8171$, $c = 8.2048$ Å. The structure is essentially as described by Ahtee *et al.*,³ the present refinement affording slightly higher precision than in that earlier study.

Orthorhombic structure (*Cmcm*)

While there is no obvious hierarchical reason why perovskites with *Pnma* symmetry should proceed via an intermediate orthorhombic phase in their transformation to a tetragonal phase, analysis of the powder neutron-diffraction patterns

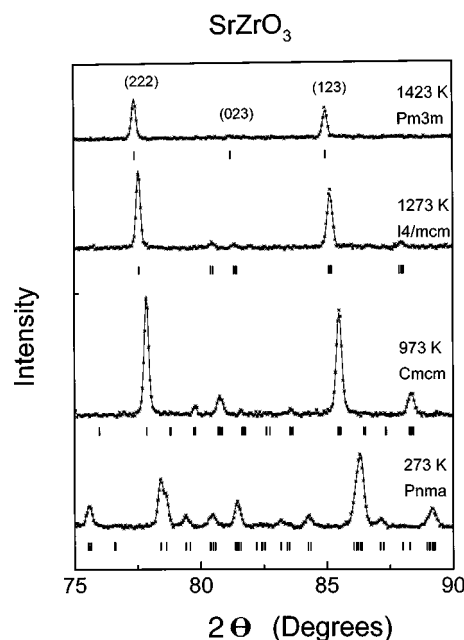


FIG. 2. Part of the powder neutron-diffraction profiles ($\lambda = 1.5005$ Å) showing the temperature dependence of some of the superlattice reflections associated with the tilted octahedra. The shift of peaks to lower angle with increasing temperature is a result of lattice expansion. In each case the solid line is that calculated by the Rietveld refinement and small vertical markers show the positions of all the allowed Bragg reflections.

shows the presence of a second orthorhombic species near 1000 K that is described in space group *Cmcm*. The refinement was undertaken using idealized starting positions and by careful and systematic variations of the various positional parameters satisfactory convergence was achieved. A critical step in obtaining a stable refinement was to initially use constraints, for example to independently refine each of the Sr and O positional parameters and to successively update these in each subsequent cycle. Attempts to simultaneously refine all the positional parameters in the early stages of the refinement were unsuccessful. In fact, there are four equivalent solutions for the structure depending on the senses of the tilts of the oxygen octahedron around that Zr atom chosen to be at the origin. We believe the initial problems with the refinement arose when the Sr atoms were displaced from their ideal position towards one of these solutions while the O atoms were displaced in an opposite sense.

In the final refinement we selected the origin to enable direct comparison with the earlier study of Ahtee, Glazer, and Hewat.⁴ All the positional parameters and anisotropic atomic displacement parameters, together with the various background and profile parameters were simultaneously varied. The results are listed in Table I. These results are in excellent agreement with the previous work and show that the ZrO_6 octahedron is axially elongated with the two O(2) atoms being ≈ 0.02 Å further from the Zr than the other four O atoms.

Tetragonal structure (*I4/mcm*)

Part of the powder neutron pattern of SrZrO_3 at 1273 K is illustrated in Fig. 2. It is clear from the pattern that a number of superlattice lines associated with the tilted oxygen octahe-

TABLE I. Structural and atomic displacement parameters ($\times 100 \text{ \AA}^2$) for orthorhombic (*Cmcm*) SrZrO₃ at 973 K.

$a = 8.2700(6) \text{ \AA}$ $b = 8.2732(6) \text{ \AA}$ $c = 8.2586(4) \text{ \AA}$							
	x	y	z	U_{11}	U_{22}	U_{33}	U_{ij}^a
Sr(1)	0	-0.0071(27)	1/4	2.2(10)	2.6(9)	1.4(6)	
Sr(2)	0	0.4897(28)	1/4	2.2(9)	4.1(13)	3.7(9)	
Zr	1/4	1/4	0	1.3(1)	1.3(1)	1.3(1)	
O(1)	0.2694(22)	0	0	3.5(8)	1.2(5)	7.7(10)	0.1(7)
O(2)	0	0.2300(25)	0.0405(15)	0.8(6)	7.0(12)	2.5(5)	0.4(5)
O(3)	0.2858(14)	0.2524(14)	1/4	2.3(5)	5.3(10)	0.4(3)	-0.1(6)

^aFor O(1) and O(2) only U_{23} has a nonzero value and for O(3) only U_{12} has a nonzero value.

dra are still present. Examination of the data showed splitting of the $12l$ type reflections indicative of tetragonal symmetry. As previously described by Ahtee and co-workers $I4/mcm$ was found to be the appropriate space group, this also being found in SrRuO₃ at 823 K,^{11,12} and in SrTiO₃ below 110 K.¹⁶ In this structure the Sr occupies the $4b$ site at $(0, 1/2, 1/4)$ and the Zr a $4c$ site at $(0,0,0)$. There are two types of oxygen atoms, O(1) at a $4a$ site at $(0, 0, 1/4)$ and O(2) on a $8h$ site at $(1/4+u, 3/4+u, 0)$. Refinement demonstrated this model to be appropriate, with appreciably better agreement between the observed and calculated profiles being obtained when anisotropic thermal parameters were employed. The final refined parameters and measures of fit are given in Table II.

At 1023 K the ZrO₆ octahedron is best described as tetragonally compressed with the axial Zr-O(1) bonds being about 0.02 Å shorter than the basal Zr-O(2) bonds 2.070 vs 2.089(3) Å. As the temperature is increased the in-plane Zr-O(2) bond distances decrease while the axial Zr-O(1) dis-

tances increase so that at 1353 K the two distances are within the precision of the structural refinements, equal 2.077 vs 2.079(3) Å. We note that at the same time the Zr-O(2)-Zr bond angle approaches 180 degrees (Table II). These results clearly demonstrate that the tilting of the ZrO₆ octahedron can induce a slight distortion, in the absence of any unusual electronic effects associated with the Zr.

A second feature of the structural refinements is the large anisotropy in the atomic displacement parameters of the O anions. These can be understood in terms of the vibration perpendicular to the Zr-O bonds being favored over bond compression. There is no evidence in these vibrations for a soft mode anomaly near the *Cmcm* to *I4/mcm* transformation.

Having obtained the cubic phase the sample was cooled again to 1223 K. As evident from Table II and Fig. 1 the cubic-tetragonal transition appears to be fully reversible, in keeping with its proposed continuous nature.

TABLE II. Structural and atomic displacement parameters ($\times 100 \text{ \AA}^2$) (ADP's) in tetragonal SrZrO₃, *I4/mcm*. The symmetry imposed constraints on the ADP for Sr, Zr, and O(1) are $U_{11}=U_{22}$ and $U_{12}=U_{13}=U_{23}=0$. For O(2) they are $U_{11}=U_{22}$ and $U_{13}=U_{23}=0$.

T (K)	1023	1073	1123	1173	1223	1273	1323	1338	1353
a (Å)	5.8456(3)	5.8498(3)	5.8506(3)	5.8569(2)	5.8577(4)	5.8617(3)	5.8665(3)	5.8676(4)	5.8697(3)
c (Å)	8.2808(5)	8.2865(6)	8.2965(5)	8.3011(3)	8.3024(7)	8.3042(5)	8.3062(6)	8.3055(9)	8.3089(7)
V (Å ³)	282.96(3)	283.47(3)	283.99(3)	284.46(2)	284.87(4)	285.32(3)	285.86(3)	285.98(4)	286.13(3)
Sr U_{11}	3.2(2)	3.7(2)	3.5(2)	3.4(1)	3.5(3)	4.0(2)	3.9(3)	4.8(4)	4.1(4)
U_{33}	2.3(3)	2.2(4)	3.3(3)	3.4(2)	3.7(5)	3.0(4)	3.7(6)	2.5(7)	3.5(8)
Zr U_{11}	2.1(2)	1.9(2)	1.5(1)	1.4(1)	1.7(2)	1.9(2)	1.8(3)	1.8(3)	2.0(3)
U_{33}	-0.1(3)	0.1(3)	1.2(3)	1.1(2)	1.0(4)	0.7(4)	1.0(5)	1.3(6)	1.0(7)
O(1) U_{11}	7.1(5)	8.5(6)	7.4(4)	7.9(3)	9.0(8)	9.6(7)	9.7(1.0)	10.0(1.3)	10.9(1.3)
U_{33}	1.1(4)	0.7(4)	1.3(3)	0.6(2)	1.1(5)	0.7(4)	0.9(5)	0.2(6)	0.1(7)
O(2) u	0.0364(6)	0.0334(6)	0.0323(5)	0.0300(4)	0.0278(9)	0.0252(7)	0.0214(8)	0.0169(9)	0.0151(9)
U_{11}	2.2(2)	2.7(2)	3.0(1)	3.2(1)	3.7(3)	3.7(2)	4.1(3)	4.3(4)	4.3(5)
U_{33}	6.7(5)	6.3(5)	6.7(4)	6.9(3)	6.6(6)	6.5(5)	7.1(7)	7.5(1.0)	7.5(1.1)
U_{12}	1.2(2)	1.5(2)	1.9(2)	2.0(1)	2.7(3)	2.4(3)	2.7(4)	2.7(5)	2.8(5)
φ (°)	8.33	7.64	7.39	6.87	6.36	5.77	4.90	3.87	3.45
Zr-O(1) (Å)	2.070(3)	2.071	2.074	2.075	2.076	2.076	2.077	2.077	2.077
Zr-O(2) (Å)	2.089(1)	2.086	2.086	2.085	2.084	2.083	2.082	2.080	2.079
Zr-O(1)-Zr	163.44	164.77	165.29	166.33	167.19	168.50	170.20	171.59	173.10
R_{Bragg} (%)	3.79	2.46	1.93	2.26	3.56	3.37	2.16	3.10	3.06
R_p (%)	8.81	8.67	8.31	6.03	11.79	8.57	8.52	9.76	8.67
R_{wp} (%)	10.62	10.57	10.13	7.48	14.73	10.40	10.44	11.84	10.72
χ^2	1.06	1.05	0.97	1.01	1.03	1.03	1.03	1.03	1.12

Cubic structure ($Pm\bar{3}m$)

The diffraction patterns collected at or above 1373 K do not show evidence of any superlattice reflections, Fig. 2, and consequently the structure was refined in the cubic space group $Pm\bar{3}m$ where the Zr occupies the $1a$ sites at (0,0,0), Sr $1b$ sites at (1/2, 1/2, 1/2) and the O the $3d$ sites at (1/2, 0, 0). It was observed during the refinements that considerably better agreement between the observed and calculated patterns was obtained when anisotropic rather than isotropic thermal parameters were included in the refinements. The oxygen atoms have their largest displacement amplitudes perpendicular to the linear Zr-O-Zr groups. This corresponds to the direction of the tilt observed in the $I4/mcm$ structure, and as expected for a soft-mode transition to the tetragonal phase the magnitude of this displacement decreases slightly on heating from 1373 to 1423 K. The smaller displacement along the Zr-O bonds increases slightly as the temperature is raised over a similar range. The ZrO_6 octahedron is now regular with a Zr-O bond distance of 2.077 Å.

Phase transitions

We have confirmed the presence of an intermediate orthorhombic phase (space group $Cmcm$) in $SrZrO_3$. This phase has an $a^{\circ}b^{+}c^{-}$ tilt system (using Glazer's notation¹⁷) and is necessarily obtained by first-order transition from the ambient temperature $Pbnm$ structure ($a^{+}b^{-}b^{-}$). The reason this transition must be first order is, that it involves an abrupt change from a structure with tilts around one tetrad and one diad axis ($a^{+}b^{-}b^{-}$) of the oxygen octahedron to one with tilts around two tetrad axes ($a^{\circ}b^{+}c^{-}$). Howard and Stokes¹³ in their Fig. 1 indicate that a continuous transition from $Cmcm$ to $P2_1/m(a^{+}b^{-}c^{-})$ is possible, however, we find no evidence in our diffraction studies to suggest any lower symmetry (than $Pnma$) for the ambient temperature structure.

The transitions from $Cmcm$ to $I4/mcm(a^{\circ}a^{\circ}c^{-})$ and from $I4/mcm$ to $Pm\bar{3}m(a^{\circ}a^{\circ}a^{\circ})$ are both allowed to be continuous in Landau theory¹³ and we observe a smooth variation in the cell volumes through these transitions, Fig. 1(b). The first of these transitions has not been studied in great detail in this work, but evidence suggests it is continuous.

The high-temperature transition from $I4/mcm$ to $Pm\bar{3}m$ has been studied in more detail and all the evidence indicates that it is continuous. The lattice parameters and variable oxygen position parameter show no measurable discontinuities

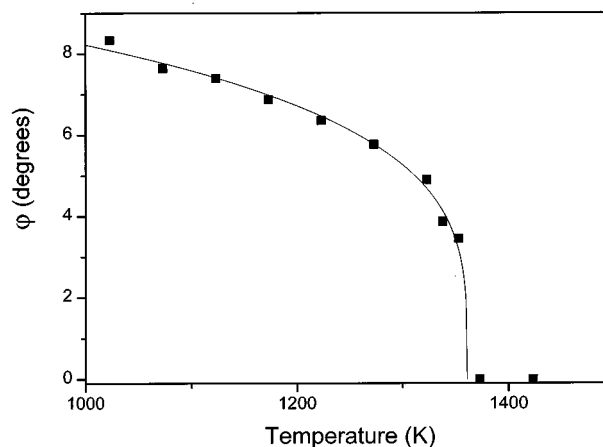


FIG. 3. Temperature dependence of the rotational angle ϕ . The fitted line is given by $\phi = A(T_c - T)^{1/4}$, with $A = 1.9$ and $T_c = 1360$ K.

and limited measurements on recooling the sample show no hysteresis. In the single tilt tetragonal phase the angle of rotation of the oxygen octahedron $\{\phi = \tan^{-1} 4u\}$ can be taken as the order parameter. The tilt angle decreases steadily as the temperature approaches the phase transition (Fig. 3), the variation with temperature being well described by $\phi \propto (T_c - T)^{1/4}$, where T_c is the transition temperature. Such variation is typical of tricritical phase transitions¹⁸ and is an indication that the coefficient of the fourth power of the order parameter in the expression for the Gibbs free energy is negligibly small. This might be a common occurrence for the tetragonal-to-cubic transition in perovskites.¹⁹ We noted above that the octahedra are not rigid, there being a 0.9% difference in the bond lengths at 1023 K, and the influence of their distortion is comparable to that of the octahedral tilting, ($1 - \cos 8.2^\circ = 1.0\%$). In these circumstances the derivation of the order parameter from the changes in the tetragonal distortion in the lattice would be quite inappropriate.

ACKNOWLEDGMENTS

Support from the Access to Major Facilities Program to carry out the work is gratefully acknowledged. Oak Ridge National Laboratory is managed by Lockheed Martin Energy Research Corporation for the U.S. Department of Energy under Contract No. DE-AC05-96OR22464.

*On leave from Australian Nuclear Science and Technology Organization, PMB 1, Menai, NSW 2234 Australia.

¹P. M. Woodward, Acta Crystallogr., Sect. B: Struct. Sci. **53**, 44 (1997).

²L. Carlsson, Acta Crystallogr. **23**, 901 (1967).

³A. Ahtee, M. Ahtee, A. M. Glazer, and A. W. Hewat, Acta Crystallogr., Sect. B: Struct. Crystallogr. Cryst. Chem. **32**, 3243 (1976).

⁴M. Ahtee, A. M. Glazer, and A. W. Hewat, Acta Crystallogr., Sect. B: Struct. Crystallogr. Cryst. Chem. **34**, 752 (1978).

⁵D. DeLigny and P. Richet, Phys. Rev. B **53**, 3013 (1996).

⁶X. Liu and R. C. Liebermann, Phys. Chem. Miner. **20**, 171 (1993).

⁷A. E. Ringwood, S. E. Kesson, K. D. Reeve, D. M. Levins, and E. J. Ramm, in *Radioactive Waste Forms for the Future*, edited by W. Lutze and R. C. Ewing (Elsevier, Amsterdam, 1988), p. 233.

⁸X. Liu, Y. Wang, and R. C. Liebermann, Geophys. Res. Lett. **15**, 1231 (1988).

⁹R. J. Hill and I. Jackson, Phys. Chem. Miner. **17**, 89 (1990).

¹⁰S. A. T. Redfern, J. Phys.: Condens. Matter **8**, 8267 (1996).

¹¹B. C. Chakoumakos, S. E. Nagler, S. T. Misture, and H. M. Christen, Physica B **241**, 358 (1997).

¹²B. J. Kennedy and B. A. Hunter, Phys. Rev. B **58**, 653 (1998).

¹³C. J. Howard and H. T. Stokes, Acta Crystallogr., Sect. B: Struct. Sci. **54**, 782 (1998).

- ¹⁴B. C. Chakoumakos, *Physica B* **241**, 361 (1997).
- ¹⁵R. J. Hill and C. J. Howard, Australian Atomic Energy Commission Research Establishment, Report No. AAEC/M112, 1986.
- ¹⁶G. Shirane and Y. Yamada, *Phys. Rev.* **177**, 858 (1969).
- ¹⁷A. M. Glazer, *Acta Crystallogr.*, Sect. B: Struct. Crystallogr. Cryst. Chem. **28**, 3384 (1972); A. M. Glazer, *Acta Crystallogr.*, Sect. A: Cryst. Phys., Diffr., Theor. Gen. Crystallogr. **31**, 756 (1975).
- ¹⁸E. K. H. Salje, *Phase Transitions in Ferroelastic and Co-elastic Crystals* (Cambridge University Press, Cambridge, 1990).
- ¹⁹M. A. Carpenter and E. K. H. Salje, *Eur. J. Mineral.* **10**, 693 (1998).